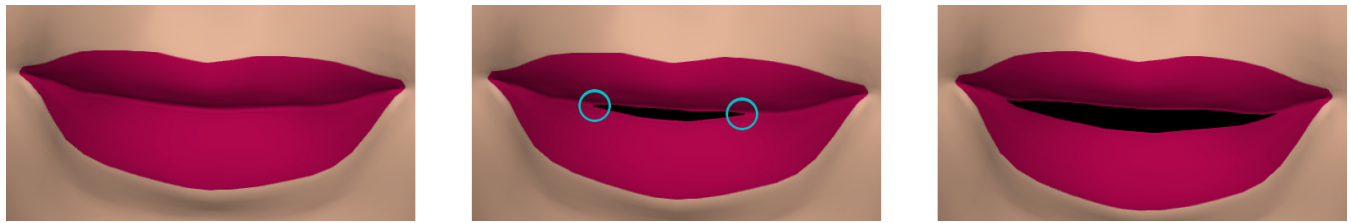


# Physically-based Sticky Lips

M. Leach<sup>1</sup> and S. Maddock<sup>1</sup>

<sup>1</sup>University of Sheffield, UK



**Figure 1:** Mouth opening with sticky lips. The ringed areas demonstrate where the lips remain in contact towards the corners of the mouth as they are drawn open. Traditional animation approaches fail to capture this behaviour.

## Abstract

In this paper, a novel solution is provided for the sticky lip problem in computer facial animation, recreating the way the lips stick together when drawn apart in speech or in the formation of facial expressions. Traditional approaches to modelling this rely on an artist estimating the correct behaviour. In contrast, this paper presents a physically-based model. The mouth is modelled using the total Lagrangian explicit dynamics finite element method, with a new breaking element modelling the saliva between the lips. With this approach, subtle yet complex behaviours are recreated implicitly, giving rise to more realistic movements of the lips. The model is capable of reproducing varying degrees of stickiness between the lips, as well as asymmetric effects.

## CCS Concepts

•Computing methodologies → Animation; Physical simulation;

## 1. Introduction

The mouth is one of the key areas in producing a convincing animation of a face, such as in visual speech applications. Humans are acutely aware of its movement. The fine details of this are therefore important to capture. One contributing factor to these movements is the stickiness of the lips, which can vary with time and position on the lips. These effects are difficult to recreate with traditional animation approaches.

The two most common techniques for animating the mouth are blend shape based approaches and using motion capture. Blend shape based approaches provide a pathway for easily creating artist directed animations. Despite this, the expressions which can be produced by such a model are limited by the extent of the blend target space. If a desired expression cannot be produced as a combination of the blend targets, the artist must create a new blend target to represent the action or expression. This can be a costly process, particularly as complex behaviours such as the sticking of the lips

may require multiple blend targets to produce even a simple set of lip sticking effects. Animations generated using marker based motion tracking also suffer from this problem – the markers are placed relatively sparsely, and are unable to capture subtle movements of areas of skin. These effects must be added in by an artist manually afterwards, which may not be accurate, and is also a time consuming process. Any editing of the animations will also require considerable work. Markerless motion tracking avoids some of these issues, since, as the surface is tracked, many finer details are captured. Despite these advantages, editing animations or morphing them to fit another creature is complex and only the visible surface is captured, meaning the behaviour of the inner surfaces of the lips, tongue and teeth must be estimated.

Physically-based animation approaches offer an alternative. These seek to model the underlying behaviour of the materials involved to reproduce realistic behaviour. Two common physically-based methods are the finite element method [DLT\* 12], used for

equilibrium analysis of solids and dynamic analysis of fluids, and particle based methods such as smoothed particle hydrodynamics which are usually used for fluid simulation [LL10]. Other physically-based models include mass-spring methods [LTW95, KHS01, ZPS01].

Our approach aims to provide the benefits of blend shape methods and motion capture techniques through the use of a physical model. By using a physically-based modelling approach, we mimic the actual behaviour of the mouth, ensuring any natural expression is reachable. The model can still be artist directed, as it is essentially parameterised by the muscle activations and physical properties of the tissues. As a result of being physically based, complex behaviours including the lips sticking and dynamic effects, which are absent or must be heuristically added to blend shape approaches, are implicitly recreated, as shown in Figure 1. This work uses the Total Lagrangian Explicit Dynamics (TLED) formulation of the Finite Element Method (FEM). This formulation of the finite element method is highly parallel, meaning a GPU can be used to generate animations using the simulation method in reasonable timeframes. The paper introduces sticky breaking elements to represent saliva. The saliva between the lips acts as a glue as it dries out, bonding the two lips through adhesive forces sticking the saliva to the lips and internal cohesive forces sticking the saliva to itself. This physically based recreation supports varying degrees of stickiness, dynamic effects as the cohesive layer breaks under tension, time varying behaviour and asymmetric effects.

The remainder of the paper is organised as follows. Section 2 gives an overview of related work, briefly introducing traditional methods of facial animation followed by a more detailed exploration of work modelling the lips. Section 3 presents the methods used in producing the results, which are given in Section 4. The results show comparisons of a model with and without stickiness evaluated against a real mouth. Finally, Section 5 gives the conclusions.

## 2. Related Work

Most work on computer facial animation has focused mainly on animation of the face as a whole. The earliest work involved only basic transformations and interpolation between certain positions [Par75]. Subsequent approaches modelled a volume rather than just the surface [Wat92, LTW95], and various approaches simulated the muscles of the face [Wat87, EF78, CP00, KHS01, SPCM97]. In more recent work, hybrid models have blended physically-based approaches with other techniques [BSC16, CBF16, KBB<sup>\*</sup>17]. The current industry standard techniques are motion capture and blendshape animation.

Motion capture techniques record the surface movement of a face from a video feed, often making use of fiducial markers. The motion can be replayed as is or adapted via a rig to animate another model [DCFN06], and is now a ubiquitous technique in the production of film animations. Marker based approaches capture the gross movement of the face well and can be easily mapped to other faces via a rig, but have trouble capturing fine details, particularly in the mouth region. Markerless methods generate a surface directly which captures the mouth movement better, although does

not capture any of the inside of the mouth [BHB<sup>\*</sup>11]. The resulting animation is hard to edit and is not very flexible as only the surface is captured.

Blendshape systems produce animations by linearly interpolating between a rest pose and various extreme poses called *blend targets*. Each blend target typically encodes one action, such as raising an eyebrow. Multiple blend targets can be used at once, producing a linear combination. Each blend target has an associated weight, controlling to what degree the blend target influences the rest pose. Mathematically, the rest pose is the vector of vertex positions,  $X$ , the blendshapes are vectors of vertex displacements,  $B_i$ , associated weights are denoted  $w_i$ , and the final animation pose,  $x'$  is given by:

$$x' = X + \sum w_i B_i \quad (1)$$

As blendshapes can only produce a linear combination of poses, rotational movements and dynamics cannot be modelled directly. In addition, the space of expressions which can be created is limited by the set of available blend targets, and there is no guarantee this space spans all desirable expressions, or is limited to physically plausible ones.

Blend forces [BSC16] are a recent alternative to blend shape based systems. Based on blend shapes, Barrielle et al. focus on encoding forces which drive a physical model of the face, rather than encoding displacements. This allows more advanced physical interactions including better lip response due to collision. The model is based on minimising nonlinear energy potentials due to elastic forces. However, it is limited by some of the same problems as blend shape based systems, notably that an expression cannot be constructed if it cannot be expressed as a combination of the available blend shapes/forces. Their system is also limited in its ability to produce more complex dynamics of skin such as wrinkling, although it does offer an improvement over blend shape based systems.

Other hybrid models have also been developed. Cong et al. [CBF16] combine a physically-based simulation with blendshapes to allow artist direction. Artists can influence the movement of particular muscles with blendshapes, whilst the remainder of the animation is completed using the physical model. Kozlov et al. [KBB<sup>\*</sup>17] also use a hybrid approach, overlaying a physical simulation on blendshape based animations, in which secondary motions caused by dynamics can be reintroduced. Ichim et al. [IKKP17] use a physics-based model with a novel muscle activation model and detect contact between the lips using axis-aligned bounding box hierarchies. This improves lip behaviour, but still does not deal with stickiness during separation of the lips.

The ‘sticky lip problem’ is a term describing the way the lips stick together due to moisture as they are drawn apart. Modelling this behaviour could improve visual realism when creating characters who are chewing, or for accurate plosive effects in visual speech, or could be used in cases where hyper-realism is required. In all cases, the only commonly available solutions are simple geometric ones such as including a corrective blend shape, or heuristic options such as creating a dynamic averaged curve between the two lips, which points are fixed to [Kim17]. In terms of academic

research, the sticking of the lips is described as ‘difficult to attain with existing real-time facial animation techniques’ [OLSL16]. Olszewski et al. approach this problem using a motion capture system which produces convincing results, but is not easy to edit for an artist. The system uses a trained convolutional neural network to learn parameters controlling a digital avatar. The Digital Emily project [ARL\*09] states that the problem has been modelled in various facial rigs, including the character Gollum in The Lord of the Rings, further demonstrating the desire for a good solution. They also include it in their project using a series of Maya deformers.

There has been limited academic work on sticky lips. They are briefly demonstrated as an example of more general work on adhesion by Gascón et al. [GZO10]. The work uses a constraint based model of adhesion and bonding, but does not give consideration to accurately modelling the lips or the way they stick. Barrielle uses spring based constraints to model sticky lips, extending his previous work on blendforces to model transient effects with a constraint based projective dynamics method [BS18]. In contrast to Barrielle’s work, our finite element method approach produces more physically realistic sticky lip behaviours, such as the continuous ‘zippering’ as the mouth opens. Our stickiness model improves on his probability based model, providing a deterministic behaviour grounded in physics. We also introduce a novel model for the level of moisture on the lips controlling the stickiness behaviour in a physically realistic manner.

In a wider context, contact and stickiness between materials have been modelled for other applications, but not with regards to the lips. For example, Chau et al. [CSS04] consider dynamic adhesive frictionless contact using a bonding field to describe the amount of material actively involved in bonding. In other areas, cohesion energies are used to guide tearing or joining between mesh segments in shape interpolation problems [ZPBK17], however, these have no physical basis. Similarly, cohesion energies are minimised to provide a consistent parameterisation in uv mapping by encouraging matching of edge pairs made up of common edges [PTH\*17], but this again does not attempt to deal with a particular physical behaviour. With regards to contact modelling, recent work employs hierarchical frameworks to perform multi-phase collision detection. Aragón and Molinari [AM14] use bounding spheres in conjunction with trajectory prediction to only compute more detailed collision detection when necessary. Reducing the number of collision calculations directly required can also be done through spatial partitioning [TKH\*05].

### 3. Methods

This section starts with an overview of the creation of the model, followed by a description of the TLED finite element method. Then, a summary of NiftySim [JTC\*15] and the underlying methods it uses is presented. Lastly, a detailed description of the methods used to model the saliva and sticky lip effect is given.

#### 3.1. Model Creation

The model was created from a surface generated by the software FaceGen [Sin17]. Photos of the user, in this case the first author, were loaded into the software. Particular facial features were

marked, and the software morphed a model to recreate the face of the user as closely as possible. The model consists of the polygon mesh surface of the face, a texture generated from the photos and generic models of the teeth and tongue. The neutral expression model was exported in the Wavefront .obj format and subsequently imported to the 3D modelling package Blender.

In Blender, the teeth, tongue, and large portions of the face were removed to leave the lower, front half of the face. All the musculature and facial features which have major effects on the movement of the mouth are contained within this region. At this stage, different material regions were defined using Blender’s material feature, shown in Figure 2. Specifically, these are the skin, and a thin saliva layer between the lips. The model was then exported in .obj format.

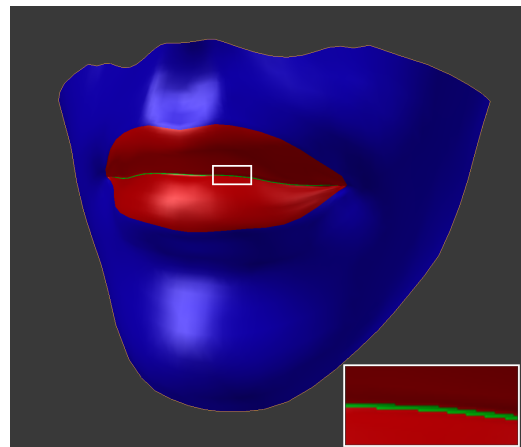


**Figure 2:** Material definitions in the modelling package Blender. Blue and red represent normal soft tissue and green represents the saliva layer.

A python script was created to extrude the quads of the mesh into hexahedra, as under-integrated linear hexahedral elements are used in the finite element simulation. This script also converts the mesh into NiftySim’s [JTC\*15] xml format.

#### 3.2. TLED method

The simulation component of the animation is conducted using the software NiftySim [JTC\*15], which is designed for soft tissue simulation. NiftySim uses the total Lagrangian explicit dynamics (TLED) formulation of the finite element method. This formulation presents various advantages for this work. A total formulation always computes timesteps relative to the initial state, allowing significant precomputation. In addition, this formulation is highly parallel as element forces can be computed in parallel – without this, the approach would be prohibitively computationally expensive on standard hardware. Many other formulations of the finite element method can not be solved in parallel in this way. The use of a dynamic formulation is essential as we are looking at producing an animation; static or quasi-static formulations aim to simulate the correct equilibrium behaviour, but do not accurately model the intermediate steps which are necessary for creating an animation rather than just a final pose.

A full analysis of the method and techniques used is available in [JTC\*15]. The fundamentals are briefly presented here. Work presented in section 3.4 onwards is novel and is implemented as an extension to NiftySim. In the total formulation, deformations are computed with respect to the initial configuration. We are also interested in large deformations. This makes the Green-Lagrange strain tensor and its work-conjugate, the second Piola-Kirchoff stress tensor, appropriate choices. From the principle of virtual work, the problem can be stated as:

$$\int_{\partial V} S \delta E dV = \int_{\partial V} \delta u f^{(B)} d^0 V + \int_{\partial S} \delta u f^{(S)} d^0 S \quad (2)$$

where  $S$  is the second Piola-Kirchoff stress tensor,  $E$  is the Green-Lagrange strain tensor,  $f^{(B)}$  is the external body force vector,  $f^{(S)}$  is the external surface force vector and  $V$  and  $S$  are the respective volume and surface on which the forces are acting. For ease of notation, the following indications have been omitted from the above equation: all instances of the stress and strain tensors are at time  $t$  with respect to the initial configuration; the body and surface force vectors are those at time  $t$ ;  $\delta u$ , the virtual displacements are also considered at time  $t$ .

This continuous domain is approximated by a series of discrete elements. Variation of physical properties over the elements is represented through shape functions. A strain-displacement matrix is used to relate strains across an element with displacements of the nodes. Through application of the prior formulae to each degree of freedom, the principle of virtual work leads to the equation of motion:

$$M^t \ddot{u} + C^t \dot{u} + k^t(u) u = r^t \quad (3)$$

where, for an element  $t$ ,  $u$  is the vector of displacements,  $M$  is the lumped (diagonal) mass matrix,  $C$  is the damping matrix,  $k^t(u)$  is the element stiffness matrix, and  $r^t$  is the external force vector.

This is solved to obtain the forces for each element using the second Piola-Kirchoff tensor:

$$f^{(e)} = 8 \det(J) \delta h S F^T \quad (4)$$

where  $f^{(e)}$  is the internal force for an element  $e$ ,  $J$  is the element Jacobian matrix,  $\delta h$  are the shape function derivatives,  $S$  is the second Piola-Kirchoff stress tensor, and  $F$  is the deformation gradient. Boundary conditions are imposed, and the simulation is advanced using the central difference integrator for time. A neo-Hookean material model is used.

### 3.3. Muscles

With the focus on recreation of the stickiness of the lips, a simple muscle model was used. Linear virtual vector muscles are used to control the mouth. Only the muscles providing the biggest effect on the movement of the mouth are modelled. Muscles are defined by an origin point, an insertion point, and a radius. Collectively these

variables define a cylinder. The forces generated by the muscle are applied to all points within the cylinder and act in a uniform direction along the length of the muscle.

### 3.4. Saliva elements

#### 3.4.1. Assumptions

Saliva has a range of rheological properties (e.g. see [Sch87]). This paper focuses on moisture level. Saliva is a complex substance made up of many things, including sugars, proteins and enzymes. When the moisture content decreases, intermolecular forces cause the saliva to become a cohesive gel, acting as a glue. A glue functions through adhesive forces between the glue and substrate, and cohesive forces binding the glue to itself [Kin12]. Our work assumes that the sticky saliva layer fails internally – the cohesive forces are weaker than the adhesive ones. As such, the saliva layer is modelled with a single layer of elements and the internal forces are used to determine when an element should break. This assumption is supported by the fact that residue can be observed on both lips when a real mouth is opened.



**Figure 3:** Shearing caused by lateral movement of the jaw.

At present, shearing forces, as illustrated in Figure 3, produced by lateral movement of the jaw, are not considered. Shearing introduces additional complexity due to the possibility of flow within the saliva layer, and the changing of where on the lip a particular saliva element might be connected to. As such, only changes in the local  $y$  direction of the element are considered, along the axis passing through the surfaces of the upper and lower lips. With the saliva layer being very thin, the saliva elements are very flat. A high stiffness is used so that they do not affect the movement of the model significantly beyond the effects of sticking the lips to each other.

#### 3.4.2. Moisture

We consider two things in the modelling of moisture for a saliva element: evaporation rate and moisture level.

The rate of evaporation of a fluid from a surface is given by the Herz-Knudsen equation:

$$\frac{1}{A} \frac{dN}{dt} \equiv \varphi = \frac{\alpha(p_{liq} - p_{eq})}{\sqrt{2\pi m k_B T_{liq}}} \quad (5)$$

where  $A$  is the surface area of the fluid,  $N$  is the number of gas molecules,  $\varphi$  is the flux of gas molecules,  $\alpha$  is a sticking coefficient for the gas molecules onto the surface,  $p_{liq}$  is the pressure of the liquid during evaporation,  $p_{eq}$  is the liquid pressure at which an equilibrium between evaporation and condensation is reached,  $m$  is the mass of a liquid particle,  $k_B$  is the Boltzmann constant and  $T_{liq}$  is the temperature of the liquid. We consider the environment and time scales under which the evaporation takes place to

further define the parameters in Equation 5. The saliva is necessarily applied to the lips from within the mouth, and thus is already at the temperature of the mouth. The saliva film is typically 0.07–0.1mm thick [CD87]. For such a small volume of fluid, the temperature would equilibrate very quickly on the surface of the lips, and the equilibrium temperature will lie between body temperature and the atmospheric temperature. A constant temperature of the lips is assumed. This means there will only be a small, fast change in saliva temperature, near instantaneous in comparison to the time scale of evaporation, so we assume the liquid temperature,  $T_{liq}$ , to be constant. We also assume the pressure difference ( $p_{liq} - p_{eq}$ ) to be constant. This gives rise to a constant evaporation rate in stable conditions, i.e. all the terms in Equation 5 are constant. However, there are other influences that can affect the evaporation rate. These are the air speed across the surface, the temperature of the surface, and changes in moisture saturation in the air surrounding the surface. The air speed and moisture saturation are both affected by the breathing cycle as air moves in and out of the body. This process is periodic, with around 16 breaths per minute on average [Pri63]. Given the short period and repetitive nature, these factors are taken as constant. Therefore, overall, a constant evaporation rate,  $\varphi$ , is used in the model, even when breathing and air-moisture saturation are taken into account.

The second thing to consider is the moisture level. For each element, an initial moisture level,  ${}^0M$ , and a current moisture level at time  $t$ ,  ${}^tM$ , are used. A moisture level of 0 represents a completely dry lip with a higher value representing more moisture. Thus, it follows that the moisture level at time  $t$  is given by:

$${}^tM = \begin{cases} {}^0M - t\varphi & \text{if } {}^0M > t\varphi \\ 0 & \text{otherwise} \end{cases} \quad (6)$$

### 3.4.3. Computing the Breaking Point

In modelling how the saliva affects the behaviour of the lips, it is important to consider two possible states for the saliva. In the first state, there is sufficient moisture that the saliva has negligible effect on the behaviour of the lips as they are drawn apart. In the second state, the saliva has dried sufficiently that it does impact on lip behaviour. To distinguish these two states, we introduce a critical moisture level,  $M_c$ , at which the saliva begins to cause stickiness between the lips.

Whether or not a saliva element should break is determined by evaluating how much the element has stretched along its y axis. This is used as a metric as it is computationally simple and, with all the elements being the same thickness, it is representative of the internal strain energy. Initially, a breaking point,  $Z$ , is determined from the moisture level,  ${}^tM$ , of the saliva element via a mapping function.

$$Z = f({}^tM, M_c) = \begin{cases} 1 & \text{if } {}^tM > M_c \\ 1 + K \frac{{}^tM}{M_c} & \text{otherwise} \end{cases} \quad (7)$$

where  $K$  is a positive coefficient describing the maximum

strength of the saliva's gluing effect. If the current moisture level,  ${}^tM$ , is above the critical moisture level,  $M_c$ , the saliva element breaks as soon as it is stretched, offering no resistance and therefore no stickiness. Below the critical moisture level, the saliva element resists stretching and generates a cohesive force between the lips.

### 3.4.4. Computing the Current Stretch

To determine the current stretch of the element, the deformation gradient of the element is computed. This is a second order tensor which maps a vector from its reference configuration to its current configuration. In the total Lagrangian formulation of the finite element method, the reference configuration is the initial configuration, that is, the configuration at time 0:

$$F_{ij} = \delta_{ij} + \frac{\partial {}^t u_i}{\partial {}^0 x_j} \quad (8)$$

where  $F$  is the deformation gradient at time  $t$ , relative to time 0,  $\delta_{ij}$  is the Kronecker delta,  ${}^t u$  gives the displacements at time  $t$ , and  ${}^0 x$  gives the initial positions. The global displacements are first transformed into a local coordinate system, so the initial orientation of the element in global space does not affect the deformation gradient.

From the deformation gradient, the right Cauchy-Green deformation tensor is computed. This tensor is rotation-invariant and physically gives the square of the change in lengths due to deformation.

$$C_{ij} = F_{ij}^T F_{ij} \quad (9)$$

where  $C$  is the right Cauchy-Green deformation tensor at time  $t$ , relative to time 0. The yy component of this tensor gives the square of the stretch in the local y direction of the undeformed finite element. This is the central component of the 3x3 tensor,  $C_{11}$ , which is used as the current stretch,  $Q$ :

$$Q = C_{11} \quad (10)$$

### 3.4.5. Force Computation

The force computation is modified to take into account whether or not the element has broken. The y-axis stretch,  $Q$ , is compared with the computed breaking point,  $Z$ , and if the element is found to be broken, the force is geometrically decreased. Unless the saliva is completely dried out, there is often a plastic style failure in which the cohesive forces decrease over time. Also, where the system is discretised into elements, a single saliva element actually represents a continuous line of saliva along the lips. With the opening of the mouth being driven by a rotation, the forces at the centre of the lips are often greater. This means it would be unusual for an entire section of the saliva to fail at once, so the force decay also helps to mimic this progressive failure. To replicate this behaviour, we



**Figure 4:** A comparison of an animation produced by a finite element model without stickiness (left column), a real mouth (middle column), and a finite element model with stickiness (right column). The stickiness provides a much more realistic movement of the lips throughout the animation. Time progresses vertically down the page with a 0.04 second interval between each row.

Property	Value
Time Step	0.00001s
Total Time Simulated	1s
Hourglass Coefficient	0.075
Damping Coefficient	80
Soft Tissue Material Model	Neo-Hookean
Soft Tissue Shear Modulus	800
Soft Tissue Bulk Modulus	7000
Soft Tissue Density	1050kg/m <sup>-3</sup>
Saliva Material Model	Neo-Hookean
Saliva Shear Modulus	Breaking
Saliva Bulk Modulus	7700
Saliva Density	191000
Initial Moisture Level	1050kg/m <sup>-3</sup>
Critical Moisture Level	100
Evaporation Rate	100
Max Glue Strength	0
	0

**Table 1:** The parameters used to generate the results shown in Figures 1, 4 and 7–11.

modify the computed internal forces generated by the element if the current stretch is greater than the computed breaking point:

$${}^tF = \begin{cases} {}^tf & \text{if } Q < Z \\ 0.99 \cdot {}^{t-1}F & \text{otherwise} \end{cases} \quad (11)$$

where  ${}^tF$  is the modified internal force of an element at time  $t$ ,  ${}^tf$  is the unmodified internal force at time  $t$  (i.e. the direct result of the TLED force computation for the element) and  ${}^{t-1}F$  is the modified force from the previous timestep (i.e. once the saliva element has broken, the force generated by the element at each timestep is 0.99 times that of the previous timestep). These additions are introduced in the form of a new material type in NiftySim. At the same time, custom rendering code was written and used for visualisation, rather than NiftySim’s default renderer.

#### 4. Results

The results produced in this section were created using the parameters shown in Table 1. An evaporation rate of 0 was chosen as all the animations produced are short. The model consists of 6982 nodes, forming 3414 hexahedral elements. Vertex displacements are recorded every 100 steps to produce an animation. Video footage of the real face was captured using a Nikon D3300 camera, recording 1080p video at 60 frames per second. The first author’s mouth was used in the video capture, and this is used to compare the simulated model against.

Figure 4 demonstrates an animation produced by a finite element model without lip stickiness (left column) and with stickiness (right column). The central column shows a real mouth opening. The two animations attempt to recreate the movement from the video by lowering the jaw. All three columns begin from the first frame before the lips begin to separate. In the animation without stickiness, it can be seen that the entire lip moves as one. Without the forces binding the lips, there is nothing to prevent the internal strains of the lip from restoring the lip to its rest shape. As a result, the entire

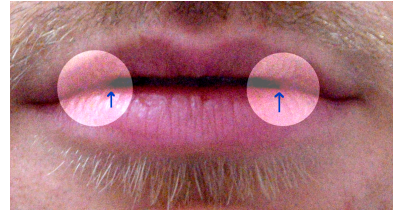


**Figure 5:** A slightly open real mouth. Note the blue arrows in the highlighted areas indicating where the lips transition from connected to separated.



**Figure 6:** Slightly open mouth position produced using blend shapes. Note the corners of the mouth being open.

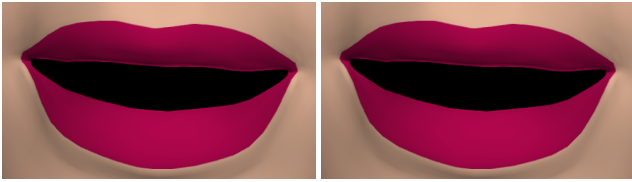
lip moves away from the upper lip in one go, creating a long, thin gap running the entire width of the lips. In the live footage of the real mouth, the lips stick together, and begin to part in the centre, with the gap being more rounded and opening up over time. The method presented in this paper successfully recreates this behaviour as seen in the right hand column. Also, the opening is asymmetric when this paper’s method is used, which matches that of the real mouth, but is absent from the model without stickiness.

Figure 5 shows a real mouth that is partially opened and the lips do not separate fully, due to stickiness. A simple blend shape approach does not produce this behaviour (Figure 6), nor does the finite element model without stickiness (Figure 7, left). Figure 7 (right) shows that the method presented in this paper captures the effect. Figure 8 shows that each FEM approach still reaches the same equilibrium position when the mouth is opened wide enough. The stickiness only affects the dynamics of the simulation.

The method presented in this paper also implicitly captures effects that are difficult to produce using a traditional blend shape approach. Figure 9 shows the lips separating in different places due to differing levels of stickiness across the lips and Figure 10 shows asymmetric opening caused by muscle activations on just one side of the face. Achieving these and other similar effects using blend shapes would require construction of new blend targets, relying on artist estimation. Even then, the dynamics producing the effects would not be accurately represented, as blend shapes are bound by interpolation, whilst the FEM based approach has a basis in reality and can deal with non-linear behaviour. To produce a segment of visual speech, with the moisture varying across the lips and a range of movements being produced, it would be infeasible to capture all the lip dynamics that might take place using blend shapes, due to the limited number of blend targets that could practically be produced. By modelling the physical behaviour of the mouth, this limitation is avoided and the model can produce any



**Figure 7:** Left: Equilibrium position generated using FEM without stickiness for a small opening of the mouth. Right: The mouth at equilibrium position having been opened the same amount with stickiness: the lips are still connected towards the edges of the mouth recreating the effect shown in the real mouth in Figure 5.



**Figure 8:** Left: Equilibrium position without stickiness. Right: Equilibrium position with stickiness. The two methods reach the same final position.

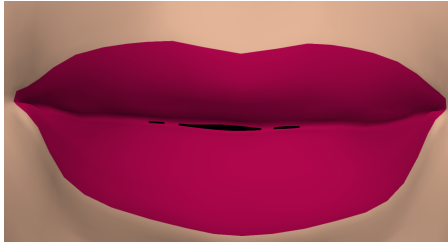


**Figure 9:** The lips can be seen separating in some places, but still stuck in places where the stickiness is higher. This would be difficult to recreate in a blend shape model but is handled here dynamically.

number of effects. It is also possible to texture map the face using standard techniques as seen in Figure 11.

## 5. Conclusions

This paper has presented a physically-based method for producing animations of the mouth incorporating lip stickiness, which produces more realistic lip behaviour than a model without stickiness. Most notably, the opening of the mouth takes place via gradual opening from the centre rather than the lips moving apart along their whole length. The model is also capable of producing effects that would be difficult to achieve using traditional facial animation techniques, such as alternating regions of the lips being stuck and unstuck, and realistic asymmetric mouth opening. The moisture model allows for natural changes of behaviour over longer periods of animation and a method for controlling the effects.

As the focus of this work has been on the stickiness of the lips, other aspects of the model have been simplified. Integration of the stickiness model with a more complete facial model remains to be done. Whilst this technique deals with simple collisions of the lips,

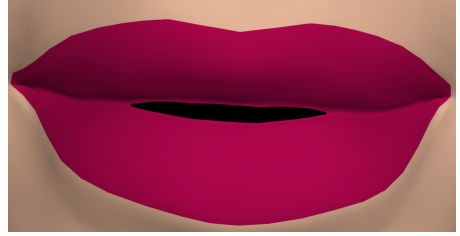


**Figure 10:** A demonstration of asymmetric opening in the mouth. This particular opening is caused by the jaw and lips being asymmetric, although similar results are seen with asymmetric muscle activation. The opening is clearly wider on one side of the mouth.



**Figure 11:** Left: Real mouth. Right: Texture mapped mouth with physically-based sticky lips.

as resistive forces are generated by compression of the saliva elements, a more rigorous model for collision between the lips could be developed. This would include shearing as the lips slide over each other. The work could also be extended to include interactions with the teeth and tongue.

## References

- [AM14] ARAGÓN A. M., MOLINARI J.-F.: A hierarchical detection framework for computational contact mechanics. *Computer Methods in Applied Mechanics and Engineering* 268 (2014), 574–588. [3](#)
- [ARL\*09] ALEXANDER O., ROGERS M., LAMBETH W., CHIANG M., DEBEVEC P.: The digital emily project: photoreal facial modeling and animation. In *ACM Siggraph 2009 courses* (2009), ACM, p. 12. [3](#)
- [BHB\*11] BEELER T., HAHN F., BRADLEY D., BICKEL B., BEARDSLEY P., GOTSMAN C., SUMNER R. W., GROSS M.: High-quality passive facial performance capture using anchor frames. *ACM Transactions on Graphics (TOG)* 30, 4 (2011), 75. [2](#)
- [BS18] BARRIELLE V., STOIBER N.: Realtime performance-driven physical simulation for facial animation. In *Computer Graphics Forum* (2018), Wiley Online Library, available online: 11 June 2018. doi: [10.1111/cgf.13450](https://doi.org/10.1111/cgf.13450). [3](#)
- [BSC16] BARRIELLE V., STOIBER N., CAGNIART C.: Blendforces: A dynamic framework for facial animation. *Computer Graphics Forum* 35, 2 (May 2016), 341–352. [2](#)
- [CBF16] CONG M., BHAT K. S., FEDKIW R.: Art-directed muscle simulation for high-end facial animation. In *Symposium on Computer Animation* (2016), pp. 119–127. [2](#)
- [CD87] COLLINS L., DAWES C.: The surface area of the adult human mouth and thickness of the salivary film covering the teeth and oral mucosa. *Journal of Dental Research* 66, 8 (1987), 1300–1302. [5](#)
- [CP00] CHABANAS M., PAYAN Y.: A 3D Finite Element Model of the Face for Simulation in Plastic and Maxillo-Facial Surgery. *Medical Image Computing and Computer-Assisted Intervention* (2000), 1068–1075. [2](#)
- [CSS04] CHAU O., SHILLOR M., SOFONEA M.: Dynamic frictionless contact with adhesion. *Zeitschrift für angewandte Mathematik und Physik ZAMP* 55, 1 (2004), 32–47. [3](#)
- [DCFN06] DENG Z., CHIANG P.-Y., FOX P., NEUMANN U.: Animating blendshape faces by cross-mapping motion capture data. In *Proceedings of the 2006 symposium on Interactive 3D graphics and games* (2006), ACM, pp. 43–48. [2](#)
- [DLT\*12] DHATT G., LEFRANĀ E., TOUZOT G., ET AL.: *Finite element method*. John Wiley & Sons, 2012. [1](#)
- [EF78] EKMAN P., FRIESEN W. V.: *Manual for the facial action coding system*. Consulting Psychologists Press, 1978. [2](#)
- [GZO10] GASCÓN J., ZURDO J. S., OTADUY M. A.: Constraint-based simulation of adhesive contact. In *Proceedings of the 2010 ACM SIGGRAPH/Eurographics Symposium on Computer Animation* (2010), Eurographics Association, pp. 39–44. [3](#)
- [IKKP17] ICHIM A.-E., KADLEČEK P., KAVAN L., PAULY M.: Phace: physics-based face modeling and animation. *ACM Transactions on Graphics (TOG)* 36, 4 (2017), 153. [2](#)
- [JTC\*15] JOHNSEN S. F., TAYLOR Z. A., CLARKSON M. J., HIPWELL J., MODAT M., EIBEN B., HAN L., HU Y., MERTZANIDOU T., HAWKES D. J., ET AL.: Niftysim: A gpu-based nonlinear finite element package for simulation of soft tissue biomechanics. *International journal of computer assisted radiology and surgery* 10, 7 (2015), 1077–1095. [3, 4](#)
- [KBB\*17] KOZLOV Y., BRADLEY D., BÄCHER M., THOMASZEWSKI B., BEELER T., GROSS M.: Enriching facial blendshape rigs with physical simulation. *Computer Graphics Forum* 36, 2 (2017), 75–84. [2](#)
- [KHS01] KAHLER K., HABER J., SEIDEL H. P.: Geometry-based Muscle Modeling for Facial Animation. *Proc of Graphics Interface* (2001), 37–46. [2](#)
- [Kim17] KIMON MATARA: Easy Sticky Lips, 2017. URL: <http://www.kimonmatara.com/maya-easy-sticky-lips/>. [2](#)
- [Kin12] KINLOCH A. J.: *Adhesion and adhesives: science and technology*. Springer Science & Business Media, 2012. [4](#)
- [LL10] LIU M., LIU G.: Smoothed particle hydrodynamics (sph): an overview and recent developments. *Archives of computational methods in engineering* 17, 1 (2010), 25–76. [2](#)
- [LTW95] LEE Y., TERZOPoulos D., WATERS K.: Realistic modeling for facial animation. In *Proceedings of the 22nd annual conference on Computer graphics and interactive techniques* (1995), ACM, pp. 55–62. [2](#)
- [OLSL16] OLSZEWSKI K., LIM J. J., SAITO S., LI H.: High-fidelity facial and speech animation for VR HMDs. *ACM Transactions on Graphics (TOG)* 35, 6 (2016), 221. [3](#)
- [Par75] PARKE F. I.: A model for human faces that allows speech synchronized animation. *Computers & Graphics* 1, 1 (1975), 3–4. [2](#)
- [Pri63] PRIBAN I.: An analysis of some short-term patterns of breathing in man at rest. *The Journal of Physiology* 166, 3 (1963), 425–434. [5](#)
- [PTH\*17] PORANNE R., TARINI M., HUBER S., PANIZZO D., SORKINE-HORNUNG O.: Autocuts: simultaneous distortion and cut optimization for UV mapping. *ACM Transactions on Graphics (TOG)* 36, 6 (2017), 215. [3](#)
- [Sch87] SCHWARZ W.: The rheology of saliva. *Journal of dental research* 66, 2\_suppl (1987), 660–666. [4](#)
- [Sin17] SINGULAR INVERSIONS: FaceGen, 2017. URL: <http://facegen.com/about.htm>. [3](#)
- [SPCM97] SCHEEPERS F., PARENT R. E., CARLSON W. E., MAY S. F.: Anatomy-Based Modeling of the Human Musculature. In *SIGGRAPH '97: ACM* (1997). [2](#)
- [TKH\*05] TESCHNER M., KIMMERLE S., HEIDELBERGER B., ZACHMANN G., RAGHUPATHI L., FUHRMANN A., CANI M.-P., FAURE F., MAGNENAT-THALMANN N., STRASSER W., VOLINO P.: Collision detection for deformable objects. *Computer Graphics Forum* 24, 1 (2005), 61–81. [3](#)
- [Wat87] WATERS K.: A muscle model for animation three-dimensional facial expression. *SIGGRAPH Computer Graphics* 21, 4 (Aug. 1987), 17–24. [2](#)
- [Wat92] WATERS K.: Physical model of facial tissue and muscle articulation derived from computer tomography data. In *Visualization in Biomedical Computing* (1992), International Society for Optics and Photonics, pp. 574–583. [2](#)
- [ZPBK17] ZHU Y., POPOVIĆ J., BRIDSON R., KAUFMAN D. M.: Planar interpolation with extreme deformation, topology change and dynamics. *ACM Transactions on Graphics (TOG)* 36, 6 (2017), 213. [3](#)
- [ZPS01] ZHANG Y., PRAKASH E. C., SUNG E.: A physically-based model with adaptive refinement for facial animation. *Computer Animation, 2001. The Fourteenth Conference on Computer Animation* (2001), 28–31. [2](#)